Journal of Solid State Chemistry 182 (2009) 1603–1610

Contents lists available at ScienceDirect

Journal of Solid State Chemistry

journal homepage: www.elsevier.com/locate/jssc

Epitaxial stabilization of (110)-layered perovskites of the $RE_2Ti_2O_7$ (RE = La, Nd, Sm, Gd) family

S. Havelia, S. Wang, K.R. Balasubramaniam, P.A. Salvador *

Department of Materials Science and Engineering, Carnegie Mellon University, 5000 Forbes Ave, Pittsburgh, PA 15213, USA

ARTICLE INFO

Article history:
Received 29 October 2008
Received in revised form
30 January 2009
Accepted 6 February 2009
Available online 5 March 2009

Keywords:
Pulsed laser deposition
Epitaxial stabilization
(110)-Layered perovskites
Pyrochlores
Ferroelectrics

ABSTRACT

Thin films of $RE_2Ti_2O_7$ (RE = La, Nd, Sm, Gd) were deposited on single crystal $SrTiO_3$ (110) substrates at 900 °C using pulsed laser deposition. X-ray diffraction (XRD) results showed sharp (00k) peaks (in θ–2θ scans) with narrow rocking curves (ω-scan peak widths of 0.4–0.9°), indicating that all compositions adopted the (110)-layered perovskite structure. While this is the stable structure for RE = La and Nd, it is metastable for RE = Sm and Gd. The metastable compounds are formed directly through epitaxial stabilization at these high temperatures and are shown to be isostructural to monoclinic $La_2Ti_2O_7$. The a, b, and c lattice parameters decreased monotonically with decreasing size of the RE cation, while the monoclinic angle remained fairly constant. The epitaxial relationship between the (110)-layered $RE_2Ti_2O_7$ films and the $SrTiO_3$(110) substrate was found by XRD and transmission electron microscopy to be $\{001\}\langle 010\rangle_{film}||\{110\}\langle 1\bar{1}0\rangle_{SrTiO_3}$. The single-phase, metastable, epitaxial, 100 nm thick films maintained the layered perovskite structure even after annealing at 900 °C for two hours in 200 Torr of oxygen.

1. Introduction

Layered perovskites having the general formula $A_2B_2O_7$ have attracted great interest for their ferroelectric and photocatalytic properties [1–9]. These compounds are the $n = 4$ members of the homologous series having the general formula $A_nB_nO_{3n+2}$, with $1 \leqslant n \leqslant \infty$ [10–17]. With respect to the parent perovskite ($n = \infty$), the $A_2B_2O_7$ structure has an extra layer of O_2 inserted along the perovskite [110] direction after every four (n) distorted perovskite units [10]. Rare earth ($A = RE$) titanates (B = Ti) and alkaline earth ($A = AE$) niobates (B = Nb) and tantalates (B = Ta) are some of the compounds that belong to this family [11–15,18,19]. Although this family of materials exhibits interesting properties, there are scant few materials known to adopt these structures [16]. It is of interest to develop synthesis methods that lead to specific compositions adopting the (110)-layered perovskite structure and/or to understand better the phase competition that exists for such compositions.

Here, we are concerned with the thin film synthesis of the $RE_2Ti_2O_7$ family in the (110)-layered perovskite structure, as a step towards understanding the utility of thin film synthesis in increasing the number of known phases to adopt this interesting structure. In the $RE_2Ti_2O_7$ family, the bulk stable structure is the (110)-layered perovskite structure when RE = La or Nd [20–22]; these we refer to as the larger rare earth titanates. The larger rare earth titanates are known to be ferroelectric with high Curie temperatures ~1500 °C [5,23]. Their temperature stability and low dielectric loss at microwave frequencies makes them attractive for high frequency applications [9]. Indeed, both $La_2Ti_2O_7$ and $Nd_2Ti_2O_7$ are used in the formulation of high K microwave dielectrics [6,24]. $La_2Ti_2O_7$ has also been found to have good piezoelectric properties with possible application as a high temperature transducer material [23]. The larger rare earth titanates (La–Nd) have been synthesized previously using different techniques; solid state processing [25], sol–gel technique [6,7,26], polymerized complex method [27], and laser heated pedestal growth [23]. $La_2Ti_2O_7$ has also been synthesized in the form of thin films using molecular beam epitaxy (MBE) [28,29] and pulsed laser deposition (PLD) [30–32].

The bulk stable structure is the pyrochlore structure for RE = Lu–Sm [33]; these shall be referred to as the smaller rare earth titanates. It should be noted that several of these materials have, however, been synthesized in the (110)-layered perovskite structure. $Sm_2Ti_2O_7$ and $Eu_2Ti_2O_7$ were synthesized in this metastable form using high pressure techniques [20,34], since for these compositions the layered phase has a smaller volume than that of the stable pyrochlore. Synthesis of even smaller rare earth titanates (with $r_{RE}^{+3} < r_{Eu}^{+3}$) in the (110)-layered perovskite structure using high pressure techniques should not work since the pyrochlore is the more dense phase for such rare earths [20,33]. A low-temperature ambient-pressure topotactic approach was used to transform $EuTiO_3$ in the perovskite structure to

* Corresponding author. Fax: +1 412 268 3113.
E-mail address: paul7@andrew.cmu.edu (P.A. Salvador).

0022-4596/$ - see front matter © 2009 Published by Elsevier Inc.
doi:10.1016/j.jssc.2009.02.025

$Eu_2Ti_2O_7$ in the (110)-layered perovskite structure [35]. This topotactic synthesis approach, which involves the low-temperature oxidation ($T<800$ °C in air) of the reduced $RETiO_3$ perovskite, did not, however, yield single phase $Gd_2Ti_2O_7$ [36]. Moreover, there are no reports of extending these techniques for the synthesis of other smaller rare earth titanates in the layered perovskite structure.

Epitaxial stabilization, in which the nucleation process during thin film deposition is controlled by selecting an appropriate substrate that favors the crystallization of a specific phase, offers an alternative route for the synthesis of complex metastable phases. Epitaxial stabilization has been used to synthesize metastable compounds of different families [37–41], most notably the perovskite oxides. Metastable compounds having dense, relatively simple crystal structures, such as the perovskite, are likely to have fewer kinetic barriers during epitaxial stabilization than open, more complex structures. We have been interested in extending the utility of epitaxial stabilization to more complex structures [42]. Here we explore its use for the synthesis of the complex (110)-layered perovskite $RE_2Ti_2O_7$ compounds.

Recently, we showed that both $La_2Ti_2O_7$ and $Sr_2Nb_2O_7$ could be formed as epitaxial thin films on commercially available $SrTiO_3$(110) single crystals [32,43], but the (001)-epitaxy of the (110)-layered perovskite structure was favored only above 900 °C. Prior work on the topotactic synthesis of $Eu_2Ti_2O_7$ demonstrated that the (110)-layered perovskite transformed to the stable pyrochlore at $T>800$ °C [35]. This implies that epitaxial stabilization of the (110)-layered perovskite structure for metastable compositions might not occur above 800 °C, since their powder analogues back convert into the pyrochlore phase at such temperatures. Nevertheless, we report here on the synthesis of $La_2Ti_2O_7$, $Nd_2Ti_2O_7$, $Sm_2Ti_2O_7$, and $Gd_2Ti_2O_7$ in the (110)-layered perovskite structure as epitaxial thin films that were deposited at 900 °C. Among these, only $La_2Ti_2O_7$ has been previously reported to be synthesized as an epitaxial film in the (110)-layered perovskite structure [28–31]. Furthermore, these films are stable at 900 °C for several hours, indicating they are robust against back-transformation, unlike bulk powders that adopt the metastable structure, opening the door for more thin film materials to be realized in this interesting crystal structure.

2. Experimental details

All films were deposited on single crystal (110)-oriented (miscut $<0.2°$) $SrTiO_3$ substrates (Crystal GmbH, Germany) that were polished using chemo-mechanical techniques to angstrom level roughnesses by the vendor. The $20\times20\times0.5$ mm $SrTiO_3$ crystals were cut into $5\times5\times0.5$ mm coupons (using a diamond wire saw and a paraphin oil lubricant), were ultrasonically cleaned in acetone and ethanol for 5 min each, and were attached to a heater plate using silver paste. Stoichiometric ceramic targets were prepared using standard solid state synthesis methods [25,33,44]. Films were deposited by PLD. Briefly, depositions were carried out at a substrate temperature of 900 °C, a laser fluence of 2 J/cm^2, a laser repetition rate of 3 Hz, and a target to substrate distance of ≈6 cm. The films were grown under a dynamic oxygen environment (1–10 mTorr O_2), which was optimized for the growth of different compounds. The dynamic pressure of oxygen had to be optimized for the growth of different compounds to suppress the nucleation of other competing phases (such as the stable pyrochlore). It was observed, especially in the growth of metastable $RE_2Ti_2O_7$ compounds, that deposition at lower rates ~0.1 Å/pulse (as determined independently by X-ray reflectivity [45]) suppressed the nucleation of the pyrochlore phase. The films were grown to a thickness ≈100 nm and were cooled down to room temperature under a static oxygen pressure of 200 Torr.

The crystalline nature (phase, crystalline quality, and epitaxial relationship) of the films was characterized using both a Rigaku (Rigaku, Japan) and a Philips X'Pert (Phillips Analytical, Netherlands) X-ray diffractometers equipped with Cu$K\alpha$ radiation; normal $\theta-2\theta$ scans were carried out on the former, while ω and ϕ scans were carried out on the latter. The Rigaku diffractometer is operated at 35 kV and 25 mA, with a step size of 0.05° and a 2 s count time. The X'Pert was operated at 45 kV and 40 mA, and uses an incident beam lens to provide parallel optics. Beam size, divergence, and noise are limited using a 2×2 mm^2 anti-scatter slit, a 0.27° Soller slit, and a graphite monochromator. Transmission electron microscopy (TEM) was carried out in both diffraction and imaging modes using a Tecnai F20 TEM at 200 kV. Samples used for the TEM study were prepared as cross sections using conventional technique, by cutting, gluing, mechanical polishing, and then by argon-ion milling until perforation occurred. HRTEM simulated images were generated with the Java electron microscopy software (JEMS), using the multi-slice model. Simulated images were calculated for wide ranges of foil thickness, objective-lens focus, incident beam convergence and defocus to permit comparison with the experimental images. Atomic coordinates of (110)-layered $La_2Ti_2O_7$ were used to simulate the HRTEM images [46].

3. Results and discussion

Figs. 1(a)–(d) show the X-ray diffraction (XRD) $\theta-2\theta$ scans for the $RE_2Ti_2O_7$ films, $RE=$ (a) La, (b) Nd, (c) Sm, and (d) Gd,

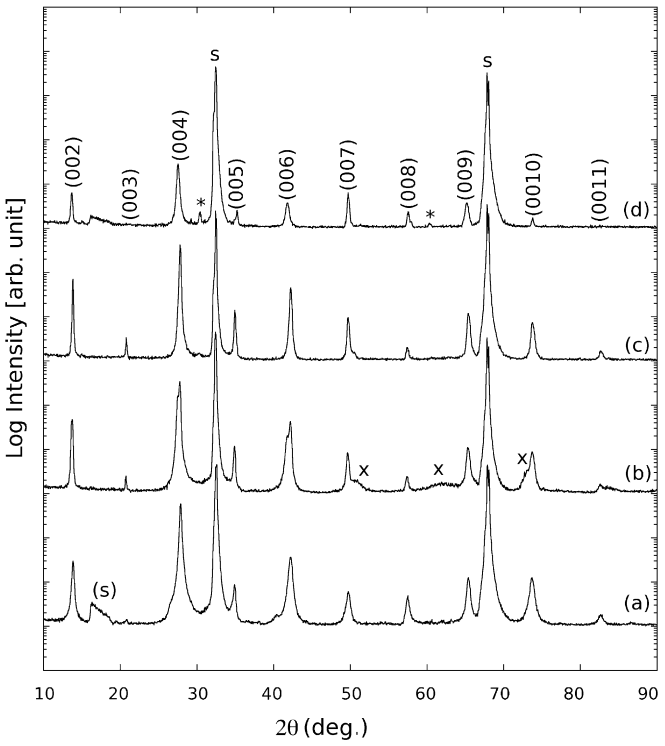

Fig. 1. Normal $\theta-2\theta$ XRD scans (shown on a log-scale, $\psi=0$) of (110)-layered perovskite $RE_2Ti_2O_7$ films on $SrTiO_3$(110) substrates: $RE=$ (a) La, (b) Nd, (c) Sm, and (d) Gd. The film peaks are marked with (00l) and the c lattice parameters are given in Table 1. The primary substrate peaks are marked 's'. A few minor peaks are observed: a substrate peak, marked as (s), appears owing to inherent defects in the substrate; two very weak {111} pyrochlore peaks have been marked with an '*'; three weak unidentified peaks are observed in the $RE=$ Nd film, marked with "x".

deposited at 900 °C on (110) $SrTiO_3$ substrates. These patterns indicate that all compositions adopted the layered perovskite structure as (00*l*)-oriented films; peaks arising from the layered perovskite are marked with the corresponding (00*l*) indices of the monoclinic structure of $La_2Ti_2O_7$. The other major peaks observed are the (*hh*0) peaks of the substrate (whose major peaks are marked with '*s*' and whose minor, defect-related peak is marked with (*s*)). Films whose patterns are shown in Fig. 1 were deposited in optimized oxygen pressures of (a) 10, (b) 1, (c) 5, and (d) 5 mTorr. These pressures led to preferential (00*l*) orientation of the layered perovskite structure and avoided the observation of the pyrochlore phase, consistent with hypothesis that the (110)-oriented $SrTiO_3$ substrate favors the nucleation of the layered perovskite phase in this specific orientation during the growth of the $RE_2Ti_2O_7$ (RE = Sm, Gd) films.

It should be noted that several weak intensity peaks are observed in some patterns of Fig. 1 (in addition to the extra substrate peak at 17°). Those peaks marked with x, which show up most pronounced in the RE = Nd film, belong to either unidentified phases in these systems or alternate orientations of the $RE_2Ti_2O_7$ (110)-layered perovskite structure (though these would be high-index orientations that normally do not form during epitaxial growth). The peak locations marked with a '*' in Fig. 1 indicate the locations of the most intense pyrochlore peaks that were observed for films deposited in other conditions (remember the pyrochlore is the competing polymorph for this composition): note their absence in all patterns but (d), where extremely low-intensity {111} pyrochlore peaks (note the log scale) were observed.

One expects that (00*l*)-$RE_2Ti_2O_7$ films would be the lowest energy orientation on (110)-$SrTiO_3$ substrates because the interfacial planes of the two materials share the geometric arrangement of the perovskite (110)-planes. Similar textures have been observed in $La_2Ti_2O_7$ and $Sr_2Nb_2O_7$ [29,32,43] films deposited on the same substrate. The unit cell (or growth unit) of the layered perovskite structure is fairly large (c~13 Å); therefore, high quality films are only obtained at high temperatures and low deposition rates (which is affected by the oxygen pressure during growth). As such, films here were deposited at 900 °C where these observations indicate sufficient diffusion occurs both parallel to and normal to the substrate surface to generate highly oriented films.

Figs. 2(a)–(d) show the XRD ω-scans (rocking curves) of the (004) peaks for the RE = (a) La, (b) Nd, (c) Sm, and (d) Gd films deposited on (110) $SrTiO_3$ substrates shown in Fig. 1. The full-width at half-maximum (FWHM) values are summarized in the lowest row of Table 1. The rocking curves are relatively narrow for such a complex layered compound and the FWHM value further confirm the high quality of the metastable $RE_2Ti_2O_7$ films. The FWHM value does increase with the lattice mismatch (see Table 1) between the (110)-layered perovskite $RE_2Ti_2O_7$ film and the (110) $SrTiO_3$ substrate. The increased lattice mismatch leads to a larger mosaic spread on relaxation and yields increased FWHMs for the more metastable compounds.

Fig. 3(a) shows the ϕ-scan registered from the {111} reflection of the $SrTiO_3$ substrate on which the $Sm_2Ti_2O_7$ film was grown, which serves as a reference for the orientation of the substrate on the goniometer. Two peaks separated by 180° in ϕ are observed, as expected. Figs. 3(b–e) show the ϕ-scans from the {$\bar{2}$04}reflections of the $RE_2Ti_2O_7$ layered perovskites for RE = (b) La, (c) Nd, (d) Sm,

Table 1
Lattice parameters, cell volume, and ω-scan (FWHM) values for the different (110)-layered $RE_2Ti_2O_7$ compounds.

Monoclinic	RE = La	RE = Nd	RE = Sm	RE = Gd
A (Å)	7.80	7.69	7.62	7.51
B (Å)	5.54	5.47	5.43	5.37
C (Å)	13.01	12.99	12.98	12.97
β (deg)	98.48	98.47	98.42	98.39
Volume (Å)	555.96	541.15	530.60	522.87
ω-FWHM (deg)	0.41	0.53	0.74	0.87

The lattice parameters were refined using the Unit cell program (see text).

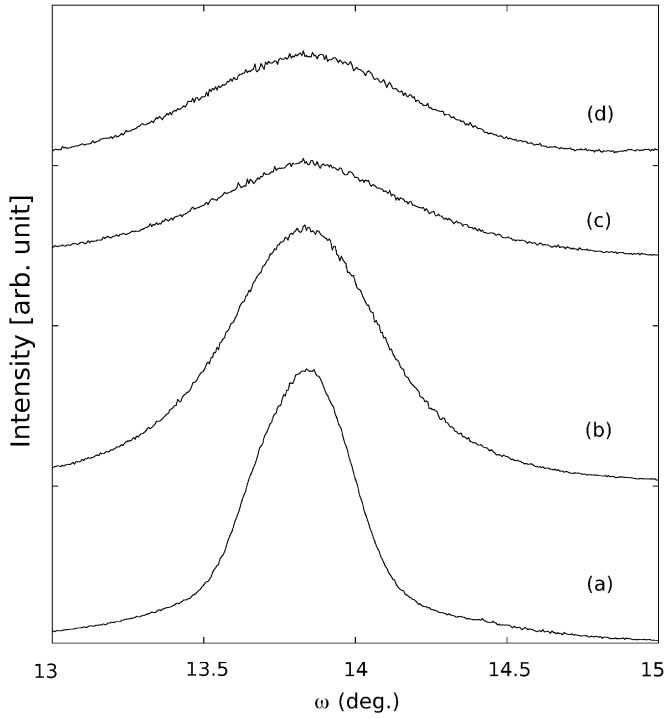

Fig. 2. XRD ω-scans for the (004) peak of the $RE_2Ti_2O_7$ films: RE = (a) La, (b) Nd, (c) Sm, and (d) Gd. FWHMs are given in Table 1.

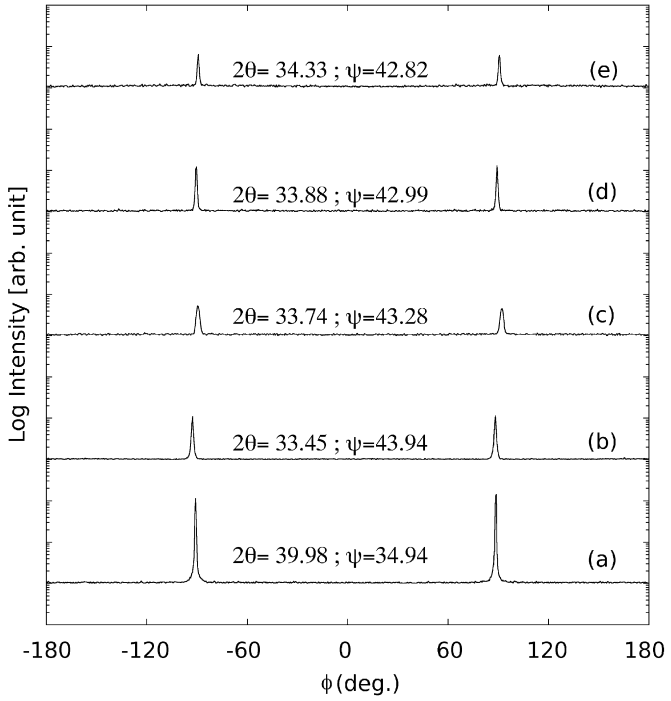

Fig. 3. XRD ϕ-scans of the (a) {111} reflections of the (110) $SrTiO_3$ substrate and (b)–(e) {$\bar{2}$04} reflections of $RE_2Ti_2O_7$ films: RE = (b) La, (c) Nd, (d) Sm, and (e) Gd. 2θ and ψ values for each case are listed.

and (e) Gd. Each of the $\{\bar{2}04\}$reflections observed in these scans were aligned with the {111} reflections of the $SrTiO_3$, although each substrate had a slightly different alignment on the goniometer, and hence slightly different ϕ values. (The film patterns given in Fig. 3 were adjusted in ϕ to properly illustrate their alignment with the substrate.) For all of the film patterns, two peaks separated by 180° in ϕ space are observed. However, only one peak should be observed if the film was composed of a single monoclinic domain. The presence of two peaks in the $\{\bar{2}04\}$ ϕ scans therefore indicates the films are epitaxial with two domains [32]. The epitaxial relationship is given by: $\{001\}_{Film}||\{110\}_{Subs} : \langle 010\rangle_{Film}||\langle 1\bar{1}0\rangle_{Subs}$, for which there are two energetically degenerate orientations, which are observed in near equal proportions for each film (Fig. 3).

Both the XRD experiments (discussed first below) and electron diffraction experiments (discussed later) demonstrate that all films adopted a monoclinic structure similar to $La_2Ti_2O_7$ ($P2_1$, $a = 7.80$ Å, $b = 5.54$ Å, $c = 13.0$ Å, $\beta = 98.6°$) [21], as opposed to the orthorhombic structure known for $Sr_2Nb_2O_7$ ($Cmc2_1$, $a = 3.93$ Å, $b = 26.7$ Å, $c = 5.68$ Å) [11]. (The two structures can be related to each other where $2^*a_{ortho} \approx a_{mono}$, $c_{ortho} \approx b_{mono}$, $b_{ortho} \approx 2^*c_{mono}$, $\beta_{mono} \approx 98°$.) XRD was used to determine the lattice parameters of the monoclinic cells, assuming all films were isostructural to $La_2Ti_2O_7$. All crystallographic indices given correspond to the monoclinic cell, unless otherwise noted.

θ–2θ X-ray scans were done around various azimuths to determine the exact 2θ positions of a number of diffraction peaks. Figs. 4(a)–(d) is one such plot that shows the XRD θ–2θ scans, around the $\{\bar{h}02h\}$ azimuth, from the $\{\bar{2}04\}$ reflections (see Fig. 3) for the RE = (a) La, (b) Nd, (c) Sm, and (d) Gd. The presence of only $\{\bar{h}02h\}$ type reflections in the θ–2θ scans further confirms the high quality epitaxy of the films. The $\{\bar{2}04\}$ reflection in the monoclinic $La_2Ti_2O_7$ cell corresponds to the (170) peak in the orthorhombic $Sr_2Nb_2O_7$ cell [11,13]. The presence of $(\bar{3}06)$ reflections, which do not have any corresponding reflections in the orthorhombic cell, confirm that the structure is monoclinic (and should be isostructural to $La_2Ti_2O_7$) and not orthorhombic (like $Sr_2Nb_2O_7$) [11]. The $(\bar{1}02)$ reflection, though present in the $La_2Ti_2O_7$ structure, has a very small intensity as compared to the other $\{\bar{h}02h\}$ reflections and, hence, is not seen in the diffraction patterns. Similarly, we observed the {403} type reflections (not shown here) in the θ–2θ scans, which also do not have any corresponding reflections in the orthorhombic cell and which further confirms that the structure is monoclinic.

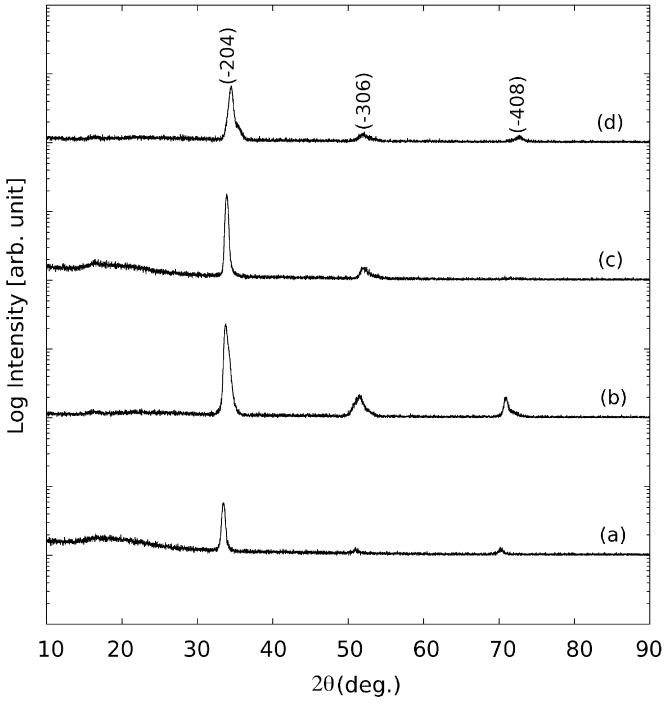

Fig. 4. XRD θ–2θ scans from the $\{\bar{2}04\}$ reflections of $RE_2Ti_2O_7$ films: RE = (a) La, (b) Nd, (c) Sm, and (d) Gd. The film peaks are marked with $(\bar{h}02h)$. The existence of the $(\bar{3}06)$ indicates the structure is monoclinic.

The lattice parameters of each of the films were determined using our X-ray observations and the Unit cell program [47], which utilizes least square refinement algorithm to best fit the collected observations to a unit cell geometry. In the range of 10–90° 2θ values, from six different families of peaks ($\{\bar{2}04\}$, $\{0\bar{2}4\}$, $\{0\bar{1}1\}$, $\{0\bar{1}3\}$, $\{2\bar{1}1\}$, and {403}) were used as inputs for the Unit cell program. The lattice parameter refinement was carried out in the monoclinic $La_2Ti_2O_7$ cell. The films were assumed to be relaxed and the effect of peak shifting due to strain was neglected in refining the lattice parameters. The refined lattice parameters are summarized in Table 1. Figs. 5(a)–(d) compare the lattice parameters and the cell volume for the different compounds obtained in this work with the bulk values previously reported in the literature [6,7,20,25–27]. The values obtained here are in good agreement with the bulk values, indicating that our films are completely relaxed. Also, the in-plane lattice parameters do not match those of the substrate, confirming that the films are relaxed from the coherently strained situation. The lattice parameters for $La_2Ti_2O_7$ (only compound reported to have been synthesized as an epitaxial film) are also in good agreement with those obtained by MBE growth [28,29]. The lattice parameters and the volume of the unit cell decrease monotonically with decreasing rare-earth size, while the monoclinic angle 'β' remains fairly constant around ≈98.4°, as summarized in Table 1.

Fig. 6 shows the results of a cross-sectional TEM study from a $Sm_2Ti_2O_7$ film. Selected area electron diffraction (SAED) patterns taken from the film's (010) zone axis and the substrate's $(1\bar{1}0)$ zone axis are shown in Figs. 6(a) and (b), respectively. The patterns can be indexed using the unit cell parameters for $Sm_2Ti_2O_7$ determined using the Unit Cell program. The SAED image clearly shows the monoclinic angle (∼98°) between the [100] and [001] film axis, which is characteristic of the $La_2Ti_2O_7$ structure and which also indicates that the film is isostructural to monoclinic $La_2Ti_2O_7$. The pattern also shows that the film is epitaxial with the $SrTiO_3$ (110) substrate and corroborates the orientation relationship obtained from XRD. Fig. 6(c) shows a high resolution TEM (HRTEM) image of the film. The inset shows the simulated HRTEM image for a $Sm_2Ti_2O_7$ film, which was generated using JEMS software. The simulated image shown was generated for a foil thickness of 20 nm and a defocus value of 15 nm. The HRTEM image reveals that the layered structure of $Sm_2Ti_2O_7$ is isostructural to monoclinic $La_2Ti_2O_7$.

The stability of the deposited films was tested by annealing films in high oxygen pressures and 900 °C for 2 h. In contrast to the topotactic growth approach [35], where impurities of the pyrochlore phase were observed after such treatments, the films maintained their structural integrity and remained single phase; in fact the crystallinity of the films (measure used was the FWHM in a ω-scan) improved on heating it to this temperature. Figs. 7(a) and (b) shows the ω-scans for the as-deposited and annealed films of $Sm_2Ti_2O_7$, respectively. The FWHM of the annealed film is ∼0.51°, smaller than the value of ∼0.74° for the as-deposited film indicating that the crystallinity of the films improved on annealing in oxygen at 900 °C.

To demonstrate that the smaller rare-earth, metastable (110)-layered perovskites were formed through epitaxial stabilization (or more precisely through a process related to the substrate surface), films were deposited on both fluorite and rock salt single

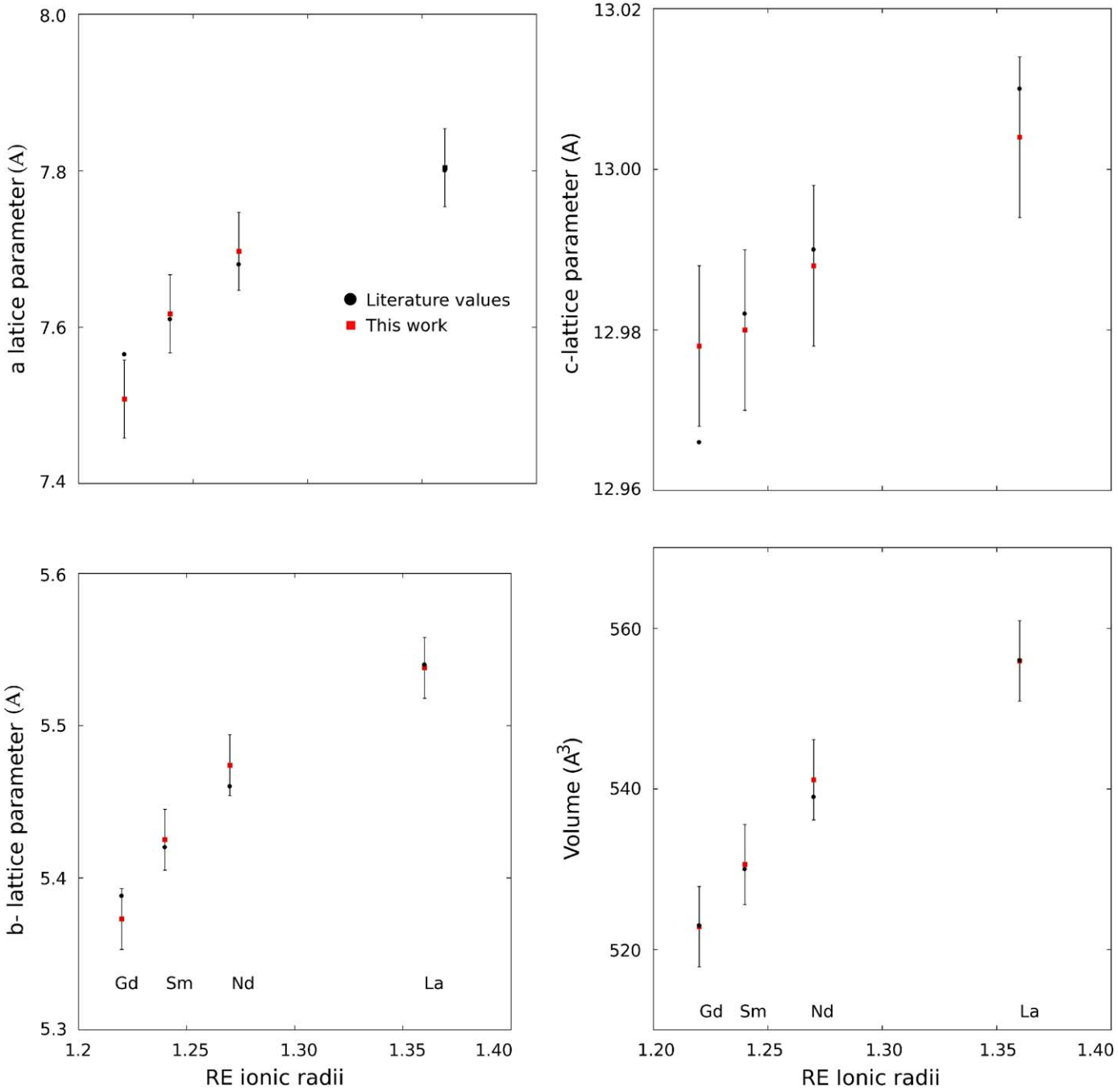

Fig. 5. Comparison of the different lattice parameters (a)–(c) and the cell volume (d), for the different $RE_2Ti_2O_7$ compounds, obtained in this work (red squares) with those previously reported in the literature (black dots). It is important to point out that the (110)-layered $Gd_2Ti_2O_7$ reported in the literature had major pyrochlore impurities [36] (for interpretation of the references to color in this figure legend, the reader is referred to the web version of this article).

crystal substrates. On a (100) fluorite substrate, i.e. yttria stabilized zirconia, it was found that epitaxial, (100)-oriented pyrochlore films were stabilized for $RE = $ Sm and Gd (X-rays not shown). This is not surprising since the pyrochlore can be considered a defect fluorite and, as such, has a good lattice match with the pyrochlore polymorph. Fig. 8 shows θ–2θ XRD scans of $RE_2Ti_2O_7$ films on MgO(111) substrates with $RE = $ (a) Sm and (b) Gd. The films are grown under the same thermodynamic conditions as the films grown on $SrTiO_3$(110) shown in Figs. 1(c) and (d) (and the YSZ(100) discussed above). Only substrate peaks (marked '*s*') and pyrochlore peaks (marked with (*hhh*)) are observed in the pattern. The growth of the bulk stable pyrochlore phase on MgO(111) indicates that the (110)-layered perovskite films are indeed epitaxially stabilized on $SrTiO_3$(110) substrates, because neither the (110)-layered perovskite nor the pyrochlore structure form a coherent interface with this MgO substrate. Importantly, what these results demonstrate is that polymorph selection for the $RE_2Ti_2O_7$ phases discussed here is controlled by substrate selection (in the growth conditions discussed here).

Our results demonstrate the good quality epitaxial films of the (110)-layered perovskite $RE_2Ti_2O_7$ ($RE = $ La, Nd, Sm, Gd) can be synthesized at 900 °C. Ideally, one could argue the thermodynamic nature of the epitaxial stabilization observed in this work. However, there is a general lack of thermodynamic data on this

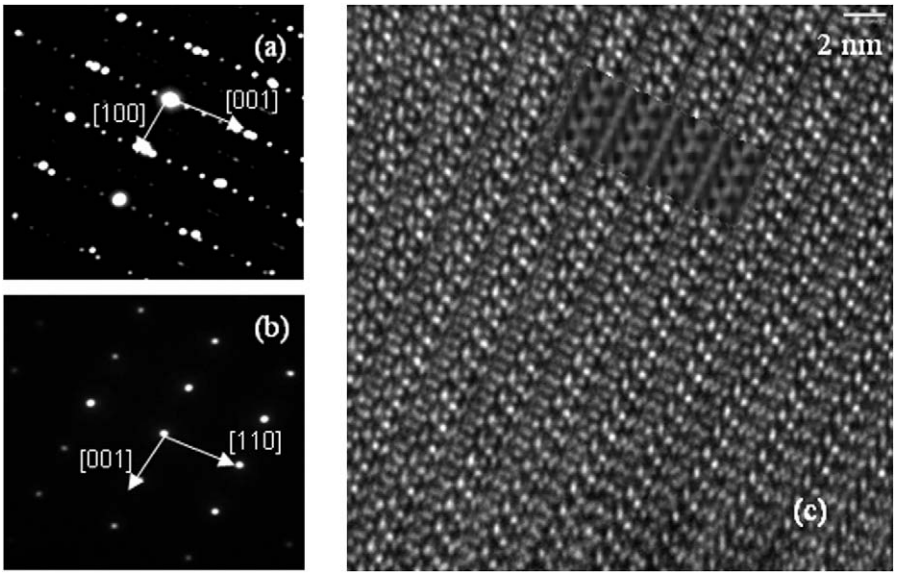

Fig. 6. Images from a cross-sectional TEM study of the $Sm_2Ti_2O_7$ film. SAED patterns from (a) the [010] zone axis of the film; (b) the [1–10] zone axis of the substrate; (c) the HRTEM image of the film along the [010] zone axis. The inset in (c) shows a simulated HRTEM image for a $Sm_2Ti_2O_7$ film, generated using JEMS software using the atom positions of $La_2Ti_2O_7$. The simulated image shown was generated for a foil thickness of 20 nm and a defocus value of 15 nm.

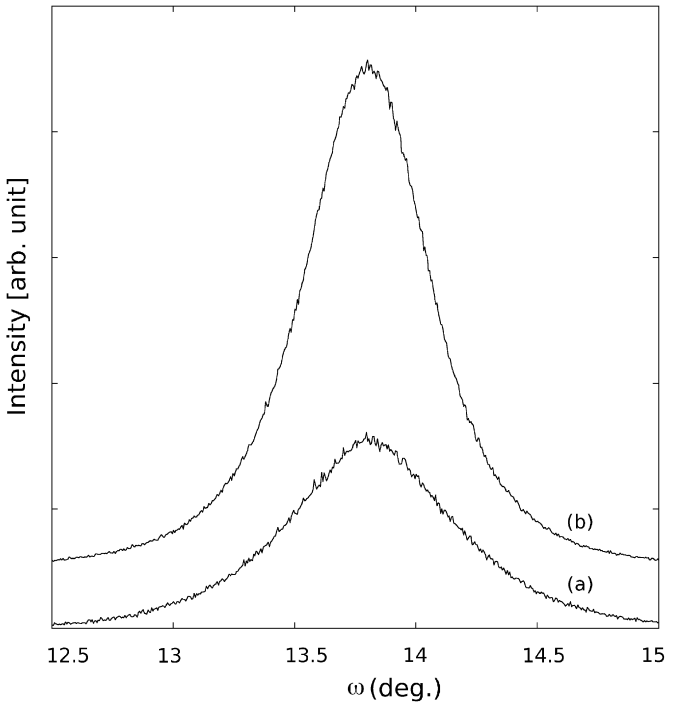

Fig. 7. XRD ω-scans for: (a) the as deposited $Sm_2Ti_2O_7$ film and (b) the $Sm_2Ti_2O_7$ films annealed in situ for 2 h at 900 °C and 200 Torr of oxygen. The increased intensity and reduced FWHM after annealing indicates the film quality improved.

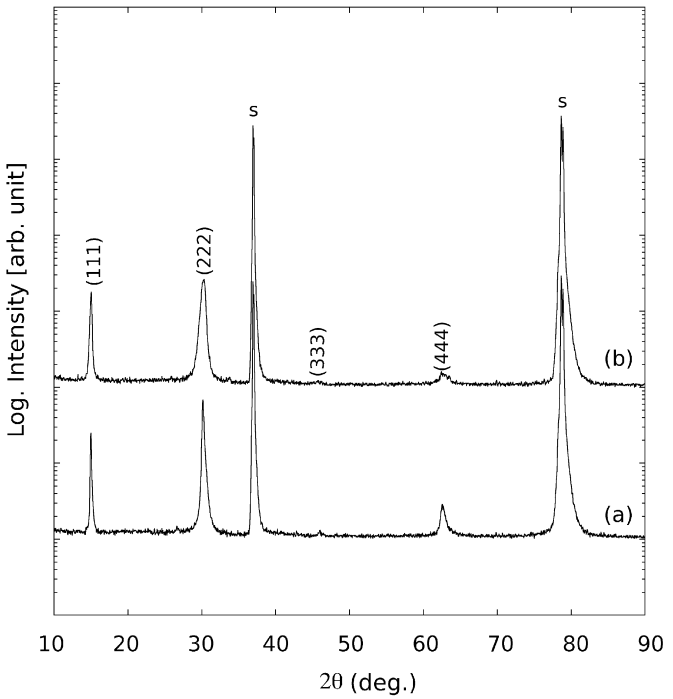

Fig. 8. θ–2θ XRD scans of pyrochlore $RE_2Ti_2O_7$ films on MgO(111) substrates with RE = (a) Sm and (b) Gd. The substrate peaks are marked 's' and the film peaks are marked with (*hhh*).

family of compounds [22]. Helean et al. calculated the heat of formation of the bulk stable $RE_2Ti_2O_7$ compounds using drop solution calorimetry [22]. Unfortunately, the enthalpy data is insufficient to make any quantitative predictions about the relative stability (which requires entropy data as well) of the two polymorphic phases. Nevertheless, by using appropriate isostructural substrates and optimizing deposition conditions we have been able to synthesize these metastable layered materials by epitaxial stabilization.

The free energy difference of the metastable layered perovskite and the stable pyrochlore phase leads to a driving force for back transformation as the films grow thicker (which reduces the importance of the substrate/film interface) or as temperature increases (which provides both increased thermal energy for kinetics and favoring the bulk stable phase). Again, owing to the lack of thermodynamic information (for both the bulk structures and the relevant interfacial energies), it is impossible to predict the thickness or temperature at which the epitaxially stabilized

materials should revert to the thermodynamically stable bulk phase. Nevertheless, 100 nm thick films of layered $Gd_2Ti_2O_7$ both nucleated and grew in the metastable structure and were stable against back transformation. Furthermore, 100 nm thick films of layered $Sm_2Ti_2O_7$ were not only more robust against back-transformation to the stable phase than bulk powders of similar metastable compounds synthesized by topochemical routes, but they improved in their crystallinity as they were annealed at 900 °C.

These collective observations indicate that the primary issue in realizing metastable (110)-layered perovskites is the prevention of the nucleation of the stable phase during growth, as seen in the growth of other metastable family of compounds [42]. These observations also imply that epitaxial stabilization is a useful synthetic approach to increase the number of known (110)-layered perovskites, although it is still of interest to understand the basic thermodynamic parameters that govern the process of epitaxial stabilization to provide some guidance towards what compositions are likely to form. Moreover, substrates that favor the growth of (110)-layered perovskites having the layered direction (the [001] in $RE_2Ti_2O_7$) in the plane of the substrate surface would allow for a significant decrease in the growth temperature (because the out-of-plane diffusion would be minimized) and could lead to improved crystal quality (similar to that observed for $YMnO_3$ layered phases [42]) and a wider stability range of specific compositions in this structure.

4. Conclusions

In conclusion, single phase epitaxial (110)-layered perovskite $RE_2Ti_2O_7$ films, RE = La, Nd, Sm, and Gd, were obtained on $SrTiO_3$ (110) substrates. $Nd_2Ti_2O_7$, $Sm_2Ti_2O_7$, and $Gd_2Ti_2O_7$ form in the (110)-layered perovskite structure as high-quality epitaxial films isostructural to monoclinic $La_2Ti_2O_7$ when deposited on (110) $SrTiO_3$ under optimized conditions. The epitaxial relationship between the substrate and films was found to be $\{001\}_{Film}||\{110\}_{Subs} : \langle 010\rangle_{Film}||\langle 1\bar{1}0\rangle_{Subs}$. In contrast to topotactic polycrystalline growth, the films maintained their structural integrity and their crystallinity improved on annealing in a high oxygen ambient at 900 °C. The films were stable against back transformation to the stable pyrochlore phase even to thicknesses of 100 nm. The films adopt crystal structures that are essentially isostructural with $La_2Ti_2O_7$ making these compounds interesting for further study for their ferroelectric properties. As the $RE_2Ti_2O_7$ compounds become increasingly metastable with decreasing RE^{+3} cation size, it would be interesting to study the limit of destabilization that can be overcome using epitaxial stabilization. Also, similar synthesis techniques can be used to obtain other metastable (110)-layered perovskite compounds in related families.

References

[1] P.T. Diallo, P. Boutinaud, R. Mahiou, J.C. Cousseins, Luminescence properties of $(La, Pr)_2Ti_2O_7$, Journal of Alloys and Compounds 275-277 (1998) 307–310.

[2] B.D. Dickerson, M. Nagata, Y.J. Song, H.D. Nam, S.B. Desu, Spectroscopic ellipsometry characterization of $La_2Ti_2O_7$ thin films, Materials Research Society Symposium Proceedings 361 (1995) 197–202.

[3] W. Kinase, S. Nanamatsu, N. Ishihara, K. Hasegawa, K. Yano, On ferroelectricity of $Sr_2Nb_2O_7$ and other $A_2B_2O_7$-type layer structure crystals, Ferroelectrics 38 (1981) 849–851.

[4] A. Kudo, H. Kato, S. Nakagawa, Water splitting into H_2 and O_2 on new $Sr_2M_2O_7$ (M = Nb and Ta) photocatalysts with layered perovskite structures: factors affecting the photocatalytic activity, Journal of Physical Chemistry B 104 (2000) 571–575.

[5] S. Nanamatsu, M. Kimura, K. Doi, S. Matsushita, N. Yamada, A new ferroelectric: $La_2Ti_2O_7$, Ferroelectrics 8 (1974) 511–513.

[6] A.V. Prasadaro, U. Selvaraj, S. Komarneni, A.S. Bhalla, Sol–gel synthesis of Ln_2 (Ln = La, Nd)Ti_2O_7, Journal of Materials Research 7 (10) (1992) 2859–2863.

[7] A.V. Prasadaro, U. Selvaraj, S. Komarneni, A.S. Bhalla, Fabrication of $La_2Ti_2O_7$ thin films by a sol–gel technique, Ferroelectrics Letters 14 (1992) 65–72.

[8] S.Y. Stefanovich, S.S. Malhasyan, Y.N. Venevtsev, Photovoltaic properties and photoconductivity of $A_2B_2O_7$ ferroelectrics, Ferroelectrics 29 (1980) 59–62.

[9] J.K. Yamamoto, A.S. Bhalla, Microwave dielectric properties of layered perovskite single crystal fibers, Materials Letters 10 (11-12) (1991) 497–500.

[10] J.K. Brandon, H.D. Megaw, On the crystal structure and properties of $Ca_2Nb_2O_7$, Philosophical Magazine 21 (1969) 189–194.

[11] N. Ishizawa, F. Marumo, T. Kawamura, M. Kimura, The crystal structure of $Sr_2Nb_2O_7$, a compound with perovskite-type slabs, Acta Crystallographica B31 (1975) 1912–1915.

[12] N. Ishizawa, F. Marumo, Compounds with perovskite-type slabs II. The crystal structure of $Sr_2Ta_2O_7$, Acta Crystallographica B32 (1976) 2564–2566.

[13] N. Ishizawa, F. Marumo, S. Iwai, M. Kimura, T. Kawamura, Compounds with perovskite type slabs. V. A high temperature modification of $La_2Ti_2O_7$, Acta Crystallographica B38 (1982) 368–372.

[14] N. Ishizawa, F. Marumo, S. Iwai, M. Kimura, S. Iwai, Compounds with perovskite type slabs. III. The structure of a monoclinic modification of $Ca_2Nb_2O_7$, Acta Crystallographica B36 (1980) 763–766.

[15] N. Ishizawa, F. Marumo, S. Iwai, Compounds with perovskite-type slabs iv. Ferroelectric phase transitions in $Sr_2(Ta_{1-x}Nb_x)_2O_7$ (x∼0.12) and $Sr_2Ta_2O_7$, Acta Crystallographica B37 (1981) 26–31.

[16] I. Levin, L.A. Bendersky, Symmetry classification of the layered perovskite-derived $A_nB_nX_{3n+2}$ structures, Acta Crystallographica B55 (1999) 853–866.

[17] I. Levin, L.A. Bendersky, T.A. Vanderah, R.S. Roth, O.M. Stafsudd, A series of incommensurately modulated $A_nB_nO_{3n+2}$ phases in the $SrTiO_3$–$Sr_2Nb_2O_7$ quasibinary system, Materials Research Bulletin 33 (3) (1998) 501–517.

[18] R.S. Roth, Pyrochlore-type compounds containing double oxides of trivalent and tetravalent ions, Journal of Research of the National Bureau of Standards 56 (1) (1956) 17–25.

[19] K. Scheunemann, H.K.M. Buschbaum, Zur Kristallstruktur Von $Ca_2Nb_2O_7$, Journal of Inorganic Nuclear Chemistry 36 (1974) 1965–1970.

[20] B. Bocquillon, F. Queyroux, C. Susse, M.R. Collongues, M.G. Chaudron, Transformation de phase sous pression du compose pyrochlore $Sm_2Ti_2O_7$, Comptes Rendus de l Academie des Sciences Paris Serie C 272 (1971) 572–575.

[21] P.M. Gasperin, Dititanate de lanthane, Acta Crystallographica B B31 (1975) 2129.

[22] K.B. Helean, S.V. Ushakov, C.E. Brown, A. Navrotsky, J. Lian, R.C. Ewing, J.M. Farmer, L.A. Boatner, Formation enthalpies of rare earth titanate pyrochlores, Journal of Solid State Chemistry 177 (2004) 1858–1866.

[23] J.K. Yamamoto, A.S. Bhalla, Piezoelectric properties of layered perovskite $A_2Ti_2O_7$ (A = La and Nd) single-crystal fibers, Journal of Applied Physics 70 (8) (1991) 4469–4471.

[24] K. Wakino, K. Minai, H. Tamura, Microwave characteristics of (zirconium, tin) titanate (Zr, Sn)TiO_4 and barium oxide lead(II) oxide–neodynium oxide–titanium dioxide dielectric resonators, Journal of the American Ceramic Society 67 (4) (1984) 278–281.

[25] P.A. Fuierer, R.E. Newnham, $La_2Ti_2O_7$ ceramics, Journal of American Ceramics Society 74 (11) (1991) 2876–2881.

[26] A.V. Prasadaro, U. Selvaraj, S. Komarneni, A.S. Bhalla, Grain orientation in sol–gel derived $Ln_2Ti_2O_7$ ceramics (Ln = La, Nd), Materials Letters 12 (1991) 306–310.

[27] M.M. Milanova, M. Kakihana, M. Arima, M. Yashima, M. Yoshimura, A simple solution route to the synthesis of pure $La_2Ti_2O_7$ and $Nd_2Ti_2O_7$ at 700–800 °C by polymerised complex method, Journal of Alloys and Compounds 242 (1996) 6–10.

[28] J.W. Seo, J. Fompeyrine, J.P. Locquet, Microstructural investigation of $La_2Ti_2O_7$ thin films grown by MBE, Superconducting and related oxides, Physics and Nanoengineering III 3481 (1998) 326.

[29] J. Fompeyrine, J.W. Seo, J.P. Locquet, Growth and characterization of ferroelectric $LaTiO_{3.5}$ thin films, Journal of the European Ceramic Society 19 (1999) 1493–1496.

[30] D. Kushkov, A.V. Zverlin, A.M. Zaslavskii, A.E. Slivinskaya, A.V. Melnikov, Structure of the $Ln_2Ti_2O_7$ thin films prepared by pulsed laser deposition, Journal of Materials Science 28 (1993) 361–363.

[31] A. Ohtomo, D.A. Muller, J.L. Grazul, H.Y. Hwang, Epitaxial growth and electronic structure of $LaTiO_x$ films, Applied Physics Letters 80 (21) (2002) 3922.

[32] S. Havelia, K.R. Balasumramaniam, S. Spurgeon, F. Cormack, P.A. Salvador, Growth of $La_2Ti_2O_7$ and $LaTiO_3$ thin films using pulsed laser deposition, Journal of Crystal Growth 310 (7-9) (2008) 1985–1990.

[33] M.A. Subramanian, G. Aravamudan, G.V. Subba Rao, Oxide pyrochlores—a review, Progressive Solid State Chemistry 15 (1983) 55–143.

[34] A.M. Sych, S.Y. Stefanovich, Y.A. Titov, T.N. Bondarenko, V.M. Melnik, $Eu_2Ti_2O_7$ phase produced at high pressures and its ferroelectric properties, Inorganic Materials 27 (12) (1992) 2229–2230.

[35] N.L. Henderson, J. Baek, P.S. Halasyamani, R.E. Schaak, Ambient-pressure synthesis of SHG-active $Eu_2Ti_2O_7$ with a [110] layered perovskite structure: suppressing pyrochlore formation by oxidation of perovskite-type $EuTiO_3$, Chemistry of Materials 19 (8) (2007) 1883.

[36] G.V. Bazuev, G.P. Shveikin, Synthesis of rare-earth titanates with the layered perovskite structure, Doklady Akademii Nauk SSSR 266 (6) (1982) 1396–1399.

[37] I.E. Graboy, A.A. Bosak, O.Y. Gorbenko, A.R. Kaul, C. Dubourdieu, J.P. Senateur, V.L. Svetchnikov, H.W. Zandbergen, HREM study of epitaxially stabilized hexagonal rare earth manganites, Chemistry of Materials 15 (2003) 2632–2637.
[38] K.R. Balasubramanian, K.C. Chang, F.A. Mohammad, L.M. Porter, P.A. Salvador, Growth and structural investigations of epitaxial hexagonal $YMnO_3$ thin films deposited on wurtzite GaN (001) substrates, Thin Solid Films 515 (4) (2006) 1807–1813.
[39] K.R. Balasubramanian, A.A. Bagal, O. Castillo, A.J. Francis, P.A. Salvador, Epitaxial phase selection in the rare earth manganite system, Ceramic Transactions 162 (2005) 59–67.
[40] A.J. Francis, A. Bagal, P.A. Salvador, Thin film synthesis of metastable perovskite: $YMnO_3$, Ceramic Transactions 115 (2000) 565–575.
[41] A.J. Francis, P.A. Salvador, Effect of surface treatment on chiral and achiral $SrTiO_3$ surface morphology and metal thin film growth, Ceramic Transactions 158 (2005) 37–46.
[42] K.R. Balasubramaniam, S. Havelia, P.A. Salvador, H. Zheng, J.F. Mitchell, Epitaxial stabilization and structural properties of REMnO3 (RE = Dy, Gd, Sm) compounds in a layered, hexagonal ABO3 structure, Applied Physics Letters 91 (23) (2007) 232901/1–232901/3.
[43] K.R. Balsubramaniam, Y. Cao, N. Patel, S. Havelia, P.J. Cox, E.C. Devlin, E.P. Yu, B.J. Close, P.M. Woodward, P.A. Salvador, Phase and structural characterization of $Sr_2Nb_2O_7$ and $SrNbO_3$ thin films grown via pulsed laser deposition in O_2 or N_2 atmospheres, Journal of Solid State Chemistry 181 (4) (2008) 705–714.
[44] F.X. Zhang, S.K. Saxena, Structural changes and pressure-induced amorphization in rare earth titanates $RE_2Ti_2O_7$ (RE: Gd, Sm) with pyrochlore structure, Chemical Physics Letters 413 (2005) 248–251.
[45] P.A. Salvador, T.D. Doan, B. Mercey, B. Raveau, Stabilization of $YMnO_3$ in a perovskite structure as a thin film, Chemistry of Materials 10 (1998) 2592–2595.
[46] H.W. Schmalle, T. Williams, A. Reller, The twin structure of $La_2Ti_2O_7$: X-ray and transmission electron microscopy studies, Acta Crystallographica B49 (1993) 235–244.
[47] T.J.B. Holland, S.A.T. Redfern, Unit cell refinement from powder diffraction data: the use of regression diagnostics, Mineralogical Magazines 61 (404) (1997) 65–77.